

# Dimensionality effects in Turing pattern formation

Teemu Leppänen, Mikko Karttunen, and Kimmo Kaski

*Laboratory of Computational Engineering,*

*Helsinki University of Technology, P.O. Box 9203, FIN-02015 HUT, Finland*

Rafael A. Barrio

*Instituto de Fisica, Universidad Nacional Autónoma de México,*

*Apartado Postal 20-364, 01000 México D.F., México*

## Abstract

The problem of morphogenesis and Turing instability are revisited from the point of view of dimensionality effects. First the linear analysis of a generic Turing model is elaborated to the case of multiple stationary states, which may lead the system to bistability. The difference between two- and three-dimensional pattern formation with respect to pattern selection and robustness is discussed. Preliminary results concerning the transition between quasi-two-dimensional and three-dimensional structures are presented and their relation to experimental results are addressed.

## I. INTRODUCTION

Alan Turing is best known for his contribution to the foundations of computer science but he has also played a key role in the birth of nonlinear dynamical theory. As he pursued his dream of artificial brain he had to concern himself with the problem of biological growth. In 1952 he published a paper, where he proposed a mechanism by which genes may determine the structure of an organism[1]. His theory did not make any new hypothesis, but it merely suggested that the fundamental physical laws can explain many of the emerging features. For example in case of a human body the problem is as follows: Can  $3 \times 10^9$  base-pairs of DNA code for approximately  $10^{11}$  neurons,  $10^{15}$  synaptic connections and estimated  $10^{13}$  cells in total? In contrast to a layman's belief that everything, i.e, structure, function and behaviour, is determined by genes, it is evident that there have to be some quite general physico-chemical mechanisms involved.

In order to develop a model for this kind of biological growth Turing was aware that he had to simplify things a lot, as becomes clear from the second sentence of his seminal paper: "This model will be a simplification and an idealization, and consequently a falsification." In order to construct a manageable model he neglected the mechanical and electrical properties of tissue, and instead considered the chemical reactions and diffusion as the crucial factors in biological growth for formulating a descriptive theory as a system of coupled reaction-diffusion equations. Turing showed that this kind of system may have a homogeneous stationary state that is unstable against perturbations. In fact, any random deviation from this stationary state leads to a symmetry break and spatial concentration patterns due to a mechanism called diffusion-driven instability. In his paper Turing discusses the blastula stage of an embryo, which appears almost spherical but shows some deviations from the perfect symmetry to different (random) directions in each embryo of a certain species. Hence he stated that they can not be of great importance to morphogenesis: "From spherical initial state chemical reactions and diffusion certainly cannot result in an organism such as a horse, which is not spherically symmetrical." Later he proved all this to be false because of the random deviations in the embryo, and stated: "It is important that there are some deviations, for the system may reach a state of instability in which these irregularities tend to grow."

The fact that all the animals of a certain species do not have exactly the same coating patterns supports Turing's idea that there is randomness involved in the morphogenesis. For example, all tigers have similar periodic patterns of stripes, but the stripes are not in the same exact positions in different tigers. Turing assumed the function of genes to be purely catalytic, and indeed the

genome is known to be the blue-print for the biological structure that is to be formed. The genes of a tiger state that it should have stripes. As a result, the genes code proteins that set the reaction and diffusion rates of the morphogens in such a way that the homogeneous state of the chemical system becomes unstable due to local or temporal inhomogeneities, which eventually lead to complex pattern formation. Here a morphogen stands for a chemical related to biological pattern formation.

These reaction-diffusion, or Turing, systems have mostly been applied in mathematical biology for explaining pattern formation in biological systems[2]. If one considers the Turing pattern of morphogens as a pre-pattern according to which the melanocytes (pigment producing cells) in the epidermis differentiate, one could explain how some animals get their nonuniform patterns. The problem is that the morphogens have not been identified *in vivo* and thus even their existence can be questioned. Yet, a lot of research has been done based on Murray's hypothesis and patterns of butterflies[3], fish[4, 5], and lady beetles[6] have been imitated by numerically solving Turing models. Apart from these numerical studies, also dynamic and stability aspects of the Turing models have been investigated[8, 9, 10]. In these, one applies the linear stability analysis or more complicated nonlinear bifurcation analysis to obtain insight of the system dynamics. Typically the parameters of a Turing model are adjusted on the basis of such an analysis. Despite the simple form of the equations theoretical analysis of the time-dependent evolution is very complicated and can only be done by analyzing the bifurcation from the stationary state. Therefore, the effect of introducing, e.g. inhomogeneous diffusion coefficients[11], growing domains[12] or curvature of the domain[13], had to be studied numerically. As other extensions of the Turing systems we have studied the formation of Turing structures in three dimensions[14], the effect of noise to Turing structures[15] and the dependence of the structural characteristics of the morphologies on the parameter selection[16]. The first experimental observation of Turing patterns was presented in 1990 in a single-phase open gel reactor with chloride-iodide-malonic acid (CIMA) reaction[17]. For a review of pattern formation in biochemical systems, we refer the reader to the extensive article by Hess[18].

In the next section of this paper we explain the idea of Turing instability in a quite general way. After that we carry out linear analysis in the case of multiple stationary states and briefly discuss the possibility of bistability in the system. The parameter selection is followed by the presentation of numerical results of two- and three-dimensional Turing systems. The differences between 2D and 3D systems are considered with respect to the pattern selection and robustness against noise. In addition, preliminary results on the transition between two and three dimensions by increasing the

thickness of the system are introduced and their connection to chemical experiments is discussed.

## II. DIFFUSION-DRIVEN INSTABILITY

Diffusion-driven instability or Turing instability is the mechanism by which the random motion of the molecules, i.e., diffusion may make a stable state of a chemical system unstable. Turing's idea of diffusion-driven instability was ground-breaking for the following reasons: 1.) It is counter-intuitive: Typically diffusion stabilizes (e.g. a droplet of ink dispersing into water due to diffusion). 2.) From any random initial state diffusion-driven instability will result in the same morphology according to intrinsic characteristics of the system (such as the random deviations in the embryo). 3.) It set the basis for research in mathematical biology, nonlinear dynamical theory and chemical pattern formation; in 1950s non-equilibrium phenomena, symmetry-breaking or complex systems were not fashionable.

The reaction-diffusion mechanism resulting in an instability was illustrated by Turing with the problem of missionaries and cannibals in an island. Missionaries come to the island by boat and want to evangelize the cannibals. The rules are as follows: If two or more missionaries meet one cannibal they can convert him to a missionary. If the relative strength is the other way around, the missionaries get killed and eaten by the cannibals. As the missionaries die, more missionaries are brought to the island. In addition, cannibals reproduce cannibals. The mechanism for instability, i.e. diffusion, is in this example the movement of cannibals and missionaries. The missionaries are assumed to have bicycles and thus they move faster, i.e., they represent the inhibitor of a reaction by slowing down the reproduction of cannibals, which in turn are the activator. Should the missionaries not have bicycles, they would always get killed as they meet cannibals, but by having bicycles they have a chance to escape and return when there are more missionaries around. With these definitions the auto-catalytic nature of the Turing mechanism becomes evident: In areas with a lot of cannibals the number of cannibals will increase due to reproduction, then being more effective in killing missionaries. On the other hand, the predominance of the cannibals means that more missionaries will be brought to the island to convert them. In most cases the cannibals and missionaries will finally find a stationary pattern, which corresponds to a map of the island where the areas with cannibal dominance can be marked by one color and the areas with missionary dominance by another color.

### III. FORMAL TURING MODELS

A Turing model describes the time variation of the concentrations of two chemical substances or morphogens due to reaction-diffusion processes. Generally a Turing system can be written as

$$\begin{aligned} U_t &= D_U \nabla^2 U + f(U, V) \\ V_t &= D_V \nabla^2 V + g(U, V), \end{aligned} \quad (1)$$

where  $U = U(\vec{r}, t)$  and  $V = V(\vec{r}, t)$  are the spatially varying concentrations, and  $D_U$  and  $D_V$  are the diffusion coefficients of the morphogens setting the time scales for the system. The reaction of the chemicals is described by the two nonlinear functions  $f$  and  $g$ , which in general can be derived from chemical reaction formulas using the law of mass action[2].

In this paper we use the generic Turing model introduced by Barrio *et al.*[5] for which the reaction kinetics is obtained by Taylor expanding the nonlinear functions around a stationary solution  $(U_c, V_c)$  defined by  $f(U_c, V_c) = 0$  and  $g(U_c, V_c) = 0$ . From Eq. (1) one can see that this condition, indeed, defines the stationary state (time derivative equal to zero) in the absence of diffusion. If terms above the third order are neglected, the equations of motion read as follows

$$\begin{aligned} u_t &= \delta D \nabla^2 u + \alpha u(1 - r_1 v^2) + v(1 - r_2 u) \\ v_t &= \delta \nabla^2 v + v(\beta + \alpha r_1 u v) + u(\gamma + r_2 v), \end{aligned} \quad (2)$$

where  $u = U - U_c$  and  $v = V - V_c$ . Terms  $r_1$  and  $r_2$  set the amplitudes of the nonlinearities, and they describe the reaction, such that quantity  $r_1$  enhances stripe formation while  $r_2$  enhances spots in two dimensions[5] and lamellae and spheres in three dimensions[14], respectively.  $D$  is the ratio of the diffusion coefficients of the two chemicals,  $\delta$  acts as a scaling factor, and  $\alpha$ ,  $\beta$  and  $\gamma$  contribute to the mode selection. Here  $D \neq 1$  is a necessary, but not sufficient condition for the diffusion-driven instability in two or more dimensions[19].

Previously, this model has been studied by setting  $\alpha = -\gamma$  to keep  $(0, 0)$  the only stationary solution[5, 14]. By relaxing this condition one can find two more stationary states defined by  $f(u_c, v_c) = g(u_c, v_c) = 0$ , reading as follows

$$u_c^i = \frac{r_2 + (-1)^i \sqrt{r_2^2 + 4\alpha r_1 (K\beta - \gamma)}}{2K\alpha r_1} \quad (3)$$

and

$$v_c^i = -K u_c^i, \quad (4)$$

where  $K = \frac{\alpha+\gamma}{1+\beta}$  and  $i = 1, 2$ .

Sufficient conditions for diffusion-driven instability to occur are widely known[2]. In our case restricting the parameter selection such that  $\alpha \in (0, 1)$ ,  $\beta \in (-1, 0)$  and  $\gamma \in (-1, 0)$  we are left with only two conditions

$$\begin{aligned} -1 < \beta < \gamma, \\ \alpha - 2\sqrt{D|\gamma|} > \beta D. \end{aligned}$$

Now the dispersion relation of the system (Eq. (2)) can be found by solving the eigenvalues of the linearized system of equations. This can be done by substituting a trial solution of the form  $w(\vec{r}, t) = \sum_k c_k e^{\lambda t} w_k(\vec{r}, t)$  into Eq. (2), which results in

$$\begin{pmatrix} \lambda u_k \\ \lambda v_k \end{pmatrix} = \begin{pmatrix} D_u & 0 \\ 0 & D_v \end{pmatrix} \begin{pmatrix} -k^2 u_k \\ -k^2 v_k \end{pmatrix} + \begin{pmatrix} f_u & f_v \\ g_u & g_v \end{pmatrix}_{u_c, v_c} \begin{pmatrix} u_k \\ v_k \end{pmatrix},$$

where  $f_u$ ,  $f_v$ ,  $g_u$  and  $g_v$  denote the partial derivatives of the reaction kinetics evaluated at the stationary state  $(u_c, v_c)$ , which in the matrix form are as follows

$$\begin{pmatrix} f_u & f_v \\ g_u & g_v \end{pmatrix}_{u_c, v_c} = \begin{pmatrix} \alpha(1 - r_1 v_c^2) - r_2 v_c & 1 - r_2 u_c - 2\alpha r_1 u_c v_c \\ \alpha r_1 v_c^2 + \gamma + r_2 v_c & \beta + 2\alpha r_1 u_c v_c + r_2 u_c \end{pmatrix}, \quad (5)$$

where  $u_c$  and  $v_c$  are given by Eqs. (3) and (4). Now the dispersion relation  $\lambda(k)$  can be solved from

$$\lambda^2 + [(D_u + D_v)k^2 - f_u - g_v] \lambda + D_u D_v k^4 - k^2(D_u f_u + D_v g_v) - f_v g_u = 0, \quad (6)$$

where  $k^2 = \vec{k} \cdot \vec{k}$  and for the generic model  $D_u = \delta D$ ,  $D_v = \delta$ .

If one chooses the parameters such that the two unstable states defined by Eqs. (3) and (4) are close to each other, preliminary numerical simulations show temporal changes in the concentration patterns as the system moves between the two stationary states. This bistability is most probably due to complex nonlinear coupling of the modes growing from the two unstable states. However, quantitative prediction of this interesting behavior requires nonlinear bifurcation analysis. The analysis and numerical results of the temporal solutions will be presented elsewhere. Following Ref. [14], we fix  $\alpha = -\gamma$  from now on.

By observing the boundaries of the region with positive growth rate, i.e.,  $\lambda(k) > 0$  one can analytically derive the modulus of the critical wave vector

$$k_c^2 = \frac{1}{\delta} \sqrt{\frac{\alpha(\beta + 1)}{D}}.$$

By adjusting the parameters and allowing only a few modes to be unstable one can end up with several different parameter sets. Here we use the parameters  $D = 0.516$ ,  $\alpha = 0.899$ ,  $\beta = -0.91$  and  $\delta = 2$ , which correspond to critical wave vector  $k_c = 0.45$  and which we have used earlier[14]. These selections fix the characteristic length of the pattern to be  $2\pi/k_c$ . The corresponding dispersion relation can be calculated based on Eq. (6), which in the case of  $u_c = v_c = 0$  reduces to

$$\lambda^2 - (\alpha + \beta - \delta k^2(1 + D))\lambda + (\alpha - \delta D k^2)(\beta - \delta k^2) - \gamma = 0. \quad (7)$$

The real part of this dispersion relation is plotted in Fig. 1. For a more detailed discussion, see Ref. [14].

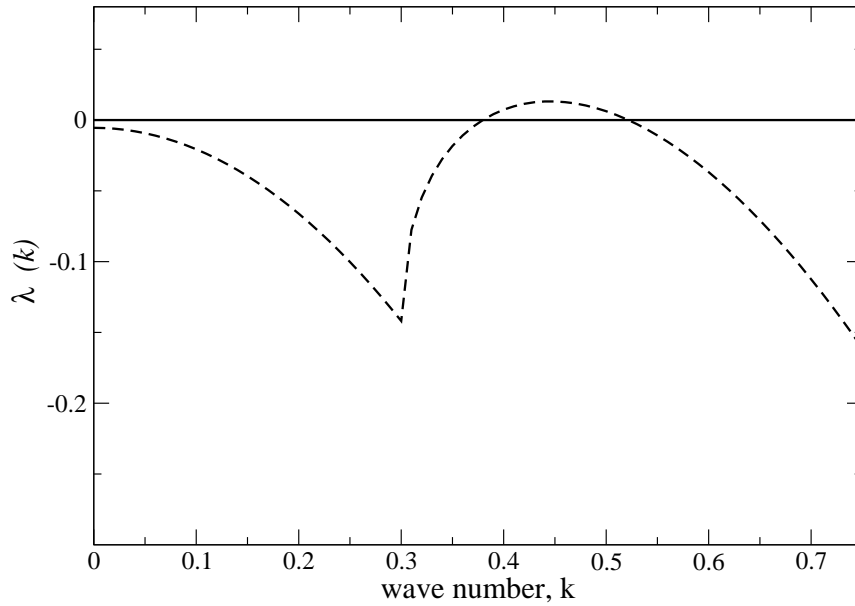


FIG. 1: The real part of dispersion relation for the critical wave vector  $k_c = 0.45$  given by Eq. (7). The unstable modes are all  $k$  for which  $\lambda(k) > 0$ .

#### IV. NUMERICAL RESULTS

The numerical simulations were carried out by discretizing the system into a spatial mesh or lattice. The Laplacian was calculated by finite difference method, with  $dx = 1.0$ , and the

equations were iterated in time using Euler's scheme with time step  $dt = 0.05$ . In a discretized three-dimensional system, the wave number values are not continuous but of the form

$$|\vec{k}| = 2\pi \sqrt{\left(\frac{n_x}{L_x}\right)^2 + \left(\frac{n_y}{L_y}\right)^2 + \left(\frac{n_z}{L_z}\right)^2}, \quad (8)$$

where  $L_{x,y,z}$  are the system dimensions to the corresponding directions and  $n_{x,y,z}$  are the wave number indices. In this paper we have used periodic boundary conditions for the concentration fields, which were initially set as random perturbations around the stationary state, i.e., random numbers with zero mean and variance of  $\sim 0.05$ .

### 2D patterns and 3D structures

In the simulations the characteristic length of the pattern is fixed by the parameter selection and the morphology of the resulting pattern can be adjusted by the nonlinear parameters  $r_1$  and  $r_2$ . The coefficient  $r_1$  of the cubic term enhances stripe or lamellae formation, whereas  $r_2$  enhances the formation of spherical shapes. Figure 2 shows the results of numerical simulations for two-dimensional  $128 \times 128$  systems, where the nonlinearities favour either spots or stripes.

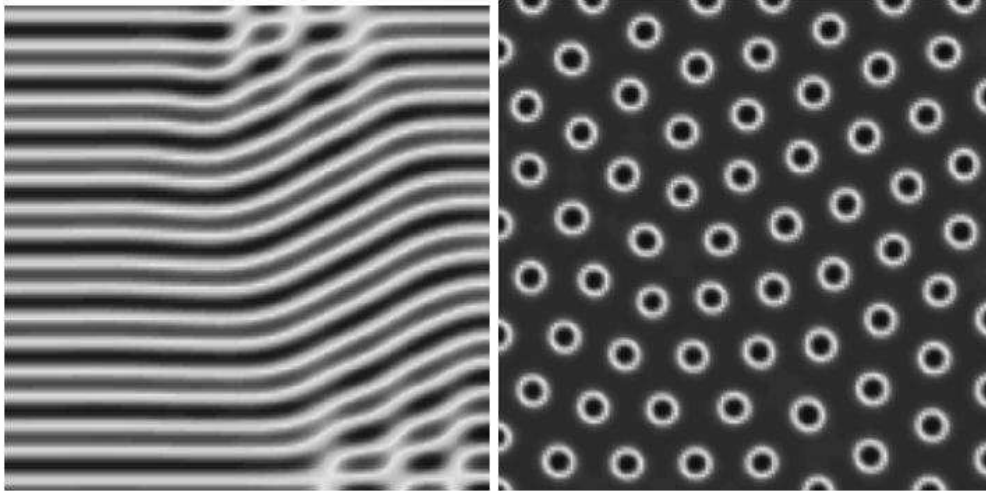


FIG. 2: The 2D patterns in a system of size  $128 \times 128$  obtained from the numerical simulation of Eq. (2). The parameters correspond to the mode  $k_c = 0.45$ . Left:  $r_1 = 3.5$  and  $r_2 = 0$ . Right:  $r_1 = 0.02$  and  $r_2 = 0.2$ .

Extending the pattern formation problem from 2D to 3D is by no means straightforward. Figure 3 shows 3D structures corresponding to the patterns of Fig. 2. The two-dimensional stripes



become complex and aligned lamellae in the three-dimensional system instead of pure lamellar planes that one would expect (see Fig. 6). This is due to one more degree of freedom. Planes are formed, but the resulting structure is, as a matter of fact, a combination of aligned planes crossing each other. The system dynamics is unable to organize the three-dimensional structure into a more regular shape. The complex lamellar structure satisfies the symmetry requirements imposed by the nonlinearities though the resulting structure is not optimal. In the case of enhanced quadratic nonlinear interaction one obtains 3D spherical shapes as one would expect (Fig. 3), but the packing is not FCC.

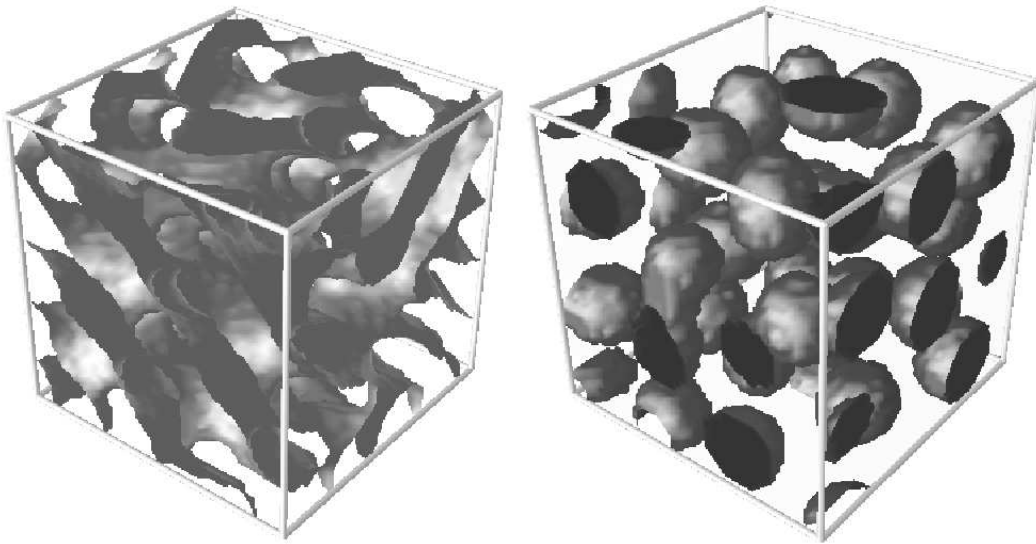


FIG. 3: The 3D structures in a system of size  $50 \times 50 \times 50$  obtained from the numerical simulation of Eq.( 2). The structure is visualized by plotting the iso-surface for one of the concentration fields. The parameters correspond to the mode  $k_c = 0.45$ . Left:  $r_1 = 3.5$  and  $r_2 = 0$ . Right:  $r_1 = 0.02$  and  $r_2 = 0.2$ .

### Dimensionality transition

The transition from 2D patterns to 3D structures is a more challenging problem than the direct comparison of the final results (Figs. 2 and 3). It has been shown experimentally that an open gel reactor with CIMA reaction may have a bistability, i.e., both spot and stripe patterns may appear into the gel on different heights. This has been explained by a concentration gradient that is imposed by the reactor[20]. Turing patterns have also been studied in ramped systems, where the thickness of the gel is increased gradually. In that case one observes qualitatively different

patterns corresponding at different thicknesses[21].

The problem has also been addressed more quantitatively by Dufiet and Boissonade[22]. They modeled the pattern formation of a three-dimensional experimental reactor by imposing a permanent gradient on one of the bifurcation parameters of their model. This corresponds to the fact that in an experimental reactor the concentrations are kept constant only on the feed surfaces, whereas the concentration inside the gel is governed by reaction and diffusion. They claim that the patterns in quasi-2D reactors can, to a certain extent, be interpreted as two-dimensional patterns when the thickness of the gel  $L_z$  is less than the characteristic wavelength  $\lambda_c = 2\pi/k_c$  of the pattern.

As for the effect of dimensionality in the generic Turing model of Eq. (2) we have observed that the transition from a 2D to a 3D system is not as simple as it has been thought. There seems to be some stochastic behaviour in the transition: As one increases the thickness of the system, it will lose the correlation between the bottom and top plates gradually, but the transition thickness is not well-defined, i.e.,  $L_z > \lambda_c$  does not guarantee that the structure becomes three-dimensional. Figure 4 shows the resulting structures for two systems of nearly the same thickness  $L_z > \lambda_c$  as one starts from random initial conditions. One can easily observe that the leftmost structures is three-dimensional, whereas the rightmost is quasi-two-dimensional, although the latter structure grows in a thicker domain. The preliminary results presented in Fig. 4 were obtained by straightforward simulations of the Lengyel-Epstein model[9], as follows

$$\begin{aligned} u_t &= \frac{1}{\sigma} \left( a - u - 4 \frac{uv}{1+u^2} + \nabla^2 u \right) \\ v_t &= b \left( u - \frac{uv}{1+u^2} \right) + d \nabla^2 v, \end{aligned} \quad (9)$$

where  $a$ ,  $b$ ,  $d$  and  $\sigma$  are adjustable parameters. We used the parameter set  $\sigma = 50$ ,  $d = 1.07$ ,  $a = 8.8$  and  $b = 0.09$ , which is known to correspond to hexagonal patterns[23].

Based on our numerical studies using both the generic Turing model (Eq. (2)) and the Lengyel-Epstein model (Eq. (9)) it seems that the probability that the pattern is three-dimensional is proportional to the number of wave vectors  $\vec{k}$  (Eq. (8)) with  $n_z \neq 0$  such that the mode  $k$  is unstable according to the dispersion relation (Eq. (7)). Our results show that the number of three-dimensional systems does not change continuously as a function of the system thickness, but the dependence is very complicated. It should also be noted that linear analysis is not sufficient to explain the complex dynamics of the dimensionality transition. Thus some sort of non-linear analysis seems necessary. However, from the numerical simulations one can calculate interesting statistics of the morphologies (e.g. correlations, structure factors), although this kind of structural analysis is diffi-

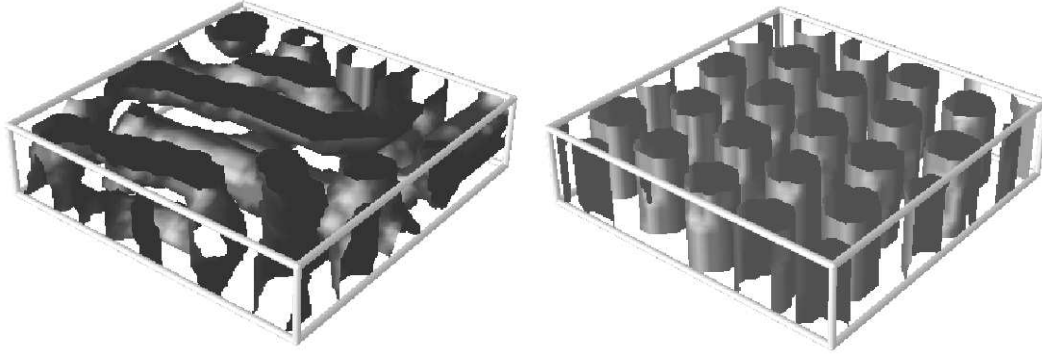


FIG. 4: Structures obtained from numerical simulation of the Lengyel-Epstein model (Eq. (9)) in a domain of size  $100 \times 100 \times L_z$ . The dimensionality of the pattern is not determined by the thickness  $L_z$  of the system alone. Left:  $L_z = 12$ . Right:  $L_z = 13$ . The system parameters are the same for both but the random initial conditions are different.

cult to carry out for chemical patterns in a gel. In addition visualization of numerical results makes it possible to see into the structure. We have used the Lengyel-Epstein model reaction[9, 23] to analyze further the structures that have been reported from experiments in ramped systems[21]. It seems that the experimental patterns can be easily misinterpreted, because the depth information is lost in the 2D projection made for visualization. What seems to be a non-harmonic modulation may be just an aligned lamellae, and what seems to be a combination of stripes and spots may as well be tubes, which appear to the observer as stripes if seen from the side and as spots if seen from the end.

As discussed above an important feature of experiments, which is absent in the numerical simulations is the gradients in the reactor. In a computer a given model can be solved to the computational precision, from which it follows that if a model captures the phenomenon accurately, the results are accurate and there are no such artifacts as concentration gradients. If one thinks of applying Turing system in biological modeling, it is of great importance that the models imitate the real processes and there is nothing that skews the results. In biological tissue the sources controlling the parameters of the reaction would in part be in the cells and not always in the boundaries. Thus the gradients are not always present in biological morphogenesis, from which it follows that the patterns obtained from numerical simulations may in fact be more realistic than the patterns arising in experimental reactors.

### The effect of noise on lamellar structures

We have recently reported results of the general Turing system concerning the effect of noise on spherical structures[15], which are more robust against noise than stripes or lamellar structures. Here we present results on the effect of noise specifically in the presence of cubic nonlinear interaction, which favours stripes or lamellae. In order to study this effect we introduce uncorrelated Gaussian noise sources  $\eta(\vec{x}, t)$  such that the equations of motion read as follows

$$\begin{aligned} u_t &= D\delta\nabla^2 u + f(u, v) + \eta_u \\ v_t &= \delta\nabla^2 v + g(u, v) + \eta_v, \end{aligned} \quad (10)$$

where the first and the second moment of the noise is defined as  $\langle\eta(\vec{x}, t)\rangle = 0$  and  $\langle\eta(\vec{x}, t)\eta(\vec{x}', t')\rangle = A^2\delta(\vec{x} - \vec{x}')\delta(t - t')$ , with the angular bracket denoting the average and  $A$  the noise intensity. It is noted that the noise was added to each lattice site at every time step of the simulation. Due to discretization the noise has to be normalized such that

$$\eta = \frac{A}{(dx)^{d/2}\sqrt{dt}}, \quad (11)$$

where  $d$  is the dimension of the system,  $dx$  the lattice constant and  $dt$  the time step.

In Figure 5 we show the two-dimensional patterns corresponding to different noise intensities for nonlinear parameters  $r_1 = 3.5$  and  $r_2 = 0$ . The noise was applied all the way throughout the evolution, and one can observe that the stripes fade into the noise gradually. It should be noted that there are complex dynamics involved in the evolution, but the patterns are still formed according to the system parameters, and even a substantial noise does not distort the evolution completely, but only makes the resulting patterns look noisy.

We have shown earlier that by using a special initial condition in the mid-plane of the system, one can obtain a three-dimensional structure of pure parallel planes[14]. Figure 6 shows such a planar structure and the same structure in the presence of noise. One can clearly see that the planes get holes on them and align even in the presence of a small amount of noise. The noise intensity in the rightmost structure of Fig. 6 corresponds to that of Fig. 5B, where the stripes are intact. This explains the fact that the three-dimensional pattern selection is very sensitive and the pure planes are not obtained from random initial conditions.

In general, we find that the three-dimensional case is much more robust against noise than the two-dimensional one, as can be observed with the help of a structure factor analysis[15]. The

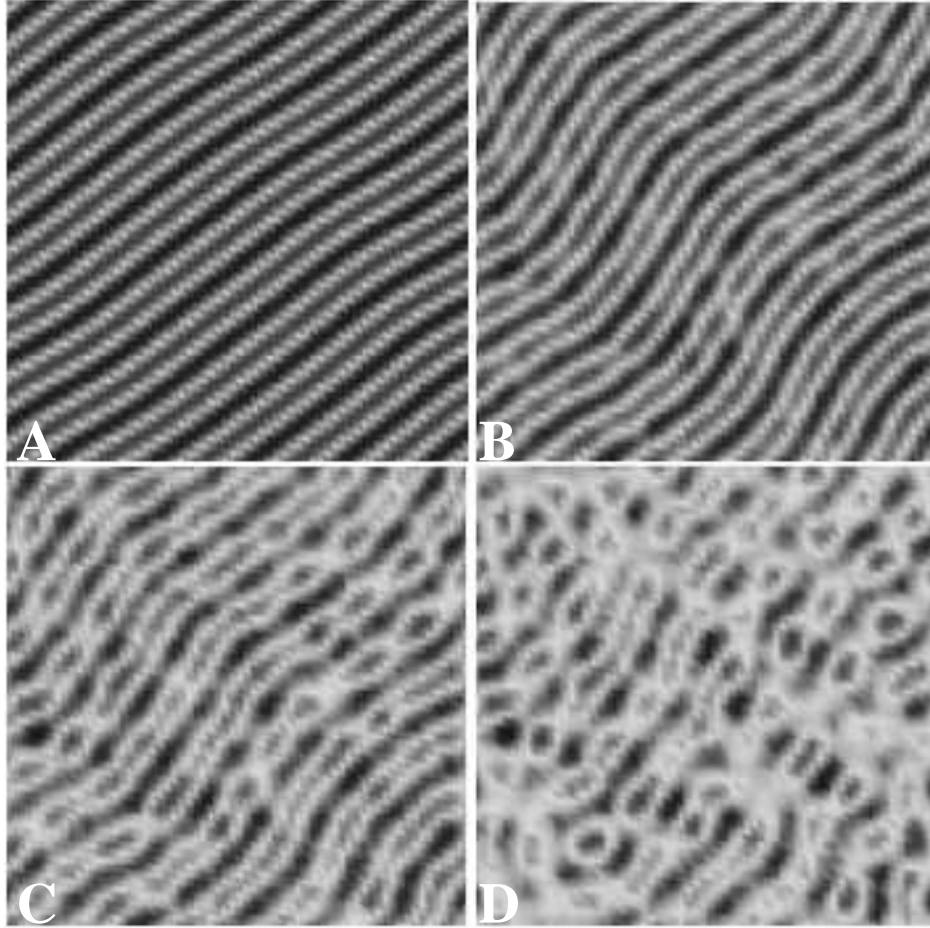


FIG. 5: Two-dimensional striped pattern in a system of size  $64 \times 64$ . The amplitude of the noise is A)  $A = 0$ , B)  $A = 0.02$ , C)  $A = 0.04$  and D)  $A = 0.06$  corresponding approximately to 0 – 40% of the amplitude of the modulated concentration wave.

interfaces of the chemical domains become distorted, but one can still localize the structure even for noise intensities up to 50% of the amplitude of the chemical concentration wave. Such high level robustness of Turing patterns is very interesting as such but also from the point of view of applying Turing systems to biological growth, in which morphogenesis seem to sustain well against external random distortions.

## V. DISCUSSION

In this paper, we have studied the characteristics of two-dimensional, quasi-two-dimensional and three-dimensional pattern formation in Turing systems. Our preliminary results indicate that

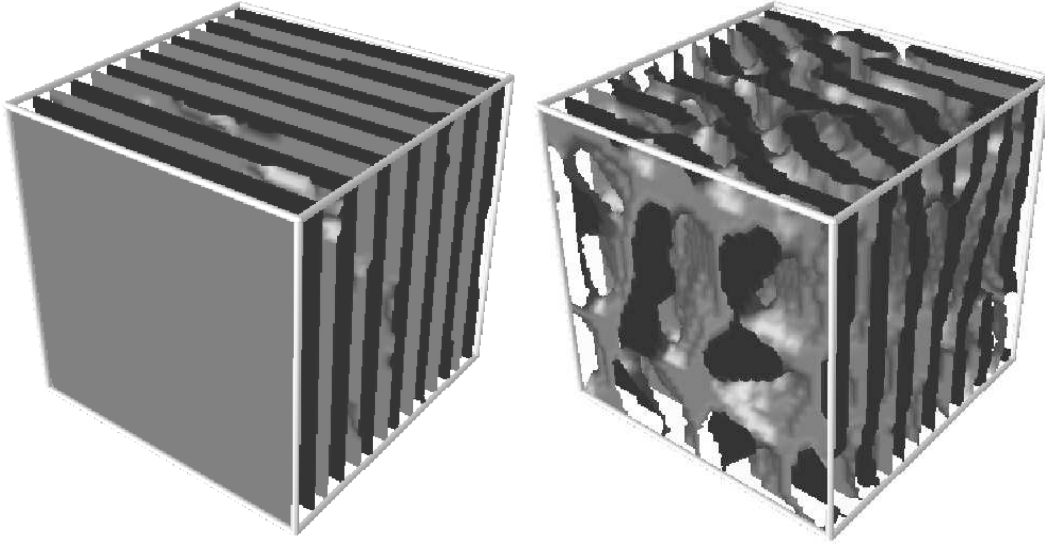


FIG. 6: Three-dimensional planar structure in a system of size  $50 \times 50 \times 50$ . The structure on the left is without noise and the one on the right with the noise amplitude  $A = 0.02$ , which corresponds approximately to 10% of the amplitude of the modulated concentration wave.

the system may behave as a three-dimensional system for certain thickness and as one *increases* the thickness, the system may behave quasi-two-dimensionally with the same set of parameters. Also we find that the pattern selection in a 3D system is much more complex than in 2D. Although spherical structures are analogous to spotty patterns, similar generalization from stripes to lamellae is not as easy. A simulation of a three-dimensional system in the presence of a cubic nonlinear interaction results in aligned lamellae with holes. This may be due to the fact that it is more difficult to maintain long-range order in three dimensions, which is required for lamellae without holes. One can observe the breaking of long-range order also in the case of spherical structures: The two-dimensional spots are organized in an almost perfect triangular lattice, whereas in 3D spherical structures seem to be unable to establish regular ordering.

In the study of the effect of noise on striped and planar structures we found that these structures and the dynamics of the instability are proportionally speaking quite robust against random perturbations. However, spherical structures can sustain more noise in absolute values since the amplitude of the concentration wave of a spherical structure is larger. We have also shown that the three-dimensional planar structure did not sustain noise as well as the corresponding two-dimensional stripe pattern although three-dimensional structures should be more robust than two-dimensional

patterns as indicated by our preliminary studies.

In this paper we have also found that the dimensionality can affect the pattern formation process in a very profound way and thus understanding the differences between two-dimensional pattern formation and three-dimensional structure formation is of great importance. The real biological processes are always taking place in a three-dimensional domain, although the symmetry restrictions, instability and dynamics governing the process may actually be quasi-two-dimensional. Therefore, choosing whether a system should be treated as three-dimensional or quasi-two-dimensional is by no means trivial and thus needing further theoretical and numerical studies for deeper understanding of morphogenesis modeling.

### Acknowledgements

One of us (R. A. B.) wishes to thank the Laboratory of Computational Engineering at Helsinki University of Technology for their hospitality. This work has been supported by the Finnish Academy of Science and Letters (T. L.) and the Academy of Finland through its Centre of Excellence Program (T. L. and K. K.).

Animations of Turing systems are available at  
<http://www.lce.hut.fi/research/polymer/turing.shtml>

- 
- [1] A.M. Turing, *Phil. Trans. R. Soc. Lond.* **B237**, 37-72 (1952).
  - [2] J.D. Murray, *Mathematical Biology*, 2nd. ed., (Springer Verlag, Berlin 1993).
  - [3] T. Sekimura, A. Madzvamuse, A.J. Wathen, and P.K. Maini, *Proceedings Royal Society London B* **267**, 851 (2000).
  - [4] S. Kondo, and R. Asai, *Nature* **376**, 678 (1995).
  - [5] R.A. Barrio, C. Varea, J.L. Aragón, and P.K. Maini, *Bull. Math. Biol.* **61**, 483 (1999).
  - [6] S.S. Liaw, C.C. Yang, R.T. Liu, and J.T. Hong, *Phys. Rev. E* **64**, 041909 (2002).
  - [7] A.L. Kawczynski and B. Legawiec, *Phys. Rev. E* **64**, 056202 (2001).
  - [8] S.L. Judd and M. Silber, *Physica D* **136**, 45 (2000).
  - [9] I. Lengyel and I. R. Epstein, *Proc. Nat. Acad. Sci.* **89**, 3977 (1992).
  - [10] T.K. Callahan and E. Knobloch, *Physica D* **132**, 339 (1999).

- [11] R.A. Barrio, J.L. Aragón, M. Torres, and P.K. Maini, *Physica D* **168-169**, 61 (2002).
- [12] C. Varea, J.L. Aragón, and R.A. Barrio, *Phys. Rev. E* **60**, 4588 (1999).
- [13] C. Varea, J.L. Aragón, and R.A. Barrio, *Phys. Rev. E* **56**, 1250 (1997).
- [14] T. Leppänen, M. Karttunen, K. Kaski, R.A. Barrio, and L. Zhang, *Physica D* **168-169**, 35 (2002).
- [15] T. Leppänen, M. Karttunen, R.A. Barrio, and K. Kaski, The effect of noise on Turing patterns, submitted 2002.
- [16] T. Leppänen, M. Karttunen, R.A. Barrio, and K. Kaski, Connectivity of Turing structures, submitted 2003. cond-mat/0302101.
- [17] V. Castets, E. Dulos, J. Boissonade and P. de Kepper, *Phys. Rev. Lett.* **64**, 2953 (1990).
- [18] B. Hess, *Quarterly Rev. Biophys.* **30**, 121 (1997).
- [19] J.A. Vastano, J.E. Pearson, W. Horsthemke, and H.L. Swinney, *Phys. Lett. A* **124**, 6 (1987).
- [20] Q. Quyang, Z. Noszticzius, and H.L. Swinney, *J. Phys. Chem.* **96**, 6773 (1992).
- [21] E. Dulos, R. Davies, B. Rudovics, and P. de Kepper, *Physica D* **98**, 53 (1996).
- [22] V. Dufiet and J. Boissonade, *Phys. Rev. E* **53**, 4883 (1996).
- [23] B. Rudovics, E. Barillot, P.W. Davies, E. Dulos, J. Boissonade, and P. de Kepper, *J. Phys. Chem.* **103**, 1790 (1999).